S-Band WDM Transmission Using PPLN-Based Wavelength Converters and 400-Gb/s C-Band Real-Time Transceivers

Tomoyuki KATO[†a], *Nonmember*, **Hidenobu MURANAKA**[†], **Yu TANAKA**[†], **Yuichi AKIYAMA**[†], *Members*,
Takeshi HOSHIDA[†], *Senior Member*, **Shimpei SHIMIZU**[††], **Takayuki KOBAYASHI**[††], **Takushi KAZAMA**[††,†††],
Takeshi UMEKI[††,†††], **Kei WATANABE**[††,†††], *Members*, **and** **Yutaka MIYAMOTO**[††], *Fellow*

SUMMARY   Multi-band WDM transmission beyond the C+L-band is a promising technology for achieving larger capacity transmission by a limited number of installed fibers. In addition to the C- and L-band, we can expect to use the S-band as the next band. Although the development of optical components for new bands, particularly transceivers, entails resource dispersion, which is one of the barriers to the realization of multi-band systems, wavelength conversion by transparent all-optical signal processing enables new wavelength band transmission using existing components. Therefore, we proposed a transmission system including a new wavelength band such as the S-band and made it possible to use a transceiver for the existing band by performing the whole-band wavelength conversion without using a transceiver for the new band. As a preliminary verification to demonstrate multi-band WDM transmission including S-band, we investigated the application of a novel wavelength converter between C-band and S-band, which consists of periodically poled lithium niobate waveguide, to the proposed system. We first characterized the conversion efficiency and noise figure of the wavelength converter and estimated the transmission performance of the system through the wavelength converter. Using the evaluated wavelength converters and test signals of 64 channels arranged in the C-band at 75-GHz intervals, we constructed an experimental setup for S-band transmission through an 80-km standard single-mode fiber. We then demonstrated error-free transmission of real-time 400-Gb/s DP-16QAM signals after forward error correction decoding. From the experimental results, it was clarified that the wavelength converter which realizes the uniform lossless conversion covering the whole C-band effectively achieves the S-band WDM transmission, and it was verified that the capacity improvement of the multi-band WDM system including the S-band can be expected by applying it in combination with the C+L-band WDM system.
key words: *optical fiber communication, optical wavelength conversion, nonlinear optics*

1. Introduction

Investment in capacity enhancement is critical to meeting the continued growth in demand for communication-based services. If the existing C and/or L bands are fully loaded, new fiber cores will need to be used additionally. However, it is not economical to keep increasing the number of fiber cores gradually, and it may be difficult to install new fibers in some areas. Multi-band wavelength-division multiplexing (WDM) transmission, which increases the number of channels accommodated by multiplexing over multiple wavelength bands beyond the C- and L-band, is an attractive solution for quickly and continuously increasing the transmission capacity of installed fibers. The study of capacity enhancement by extending the wavelength band beyond the C+L-band started around 2000 [1]–[3], but the study of the occupied wavelength band extension was suspended because the capacity improvement per channel by the digital coherent technology was achieved. However, as the capacity improvement per channel approaches the Shannon capacity limit, wavelength band extension is again attracting attention [4]–[9]. However, to take advantage of a new wavelength band in a transmission system, every optical component constituting the system must be available in the new wavelength band, which is one of the challenges for realizing a multi-band system economically. Therefore, extensive use of existing components in new wavelength bands is a candidate solution, but the performance degradation, especially at the transmitter, is inevitable [10]. To realize the transmission capacity enhancement by the wavelength band extension, it is necessary to develop a technique to overcome such wavelength limitation while avoiding an increase in the complexity of the system.

Then we are investigating all-optical wavelength conversion technology and its application to solve the constraint of the wavelength utilization extension [11]. Figure 1 illustrates an application that extends the transmission band from the supported wavelength band of a conventional WDM transceiver [12] wherein wavelength converters (C-to-L/C-to-S) for converting a conventional band signal into a long wavelength band or a short wavelength band are inserted between a WDM transmitter and a trans-
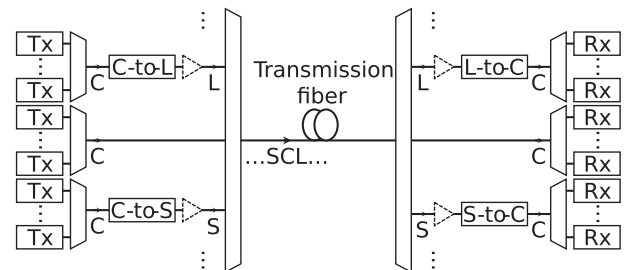
Fig. 1   Schematic diagram of a multi-band WDM transmission system using wavelength converters (C-to-L/C-to-S, L-to-C/S-to-C) and conventional band transceivers (Tx, Rx).

mission fiber input, and inverse converters (L-to-C/S-to-C) for returning the long wavelength band or short wavelength band signal to the conventional band are inserted between the transmission fiber output and a WDM receiver. By using these wavelength converters, transmission outside the conventional band is possible without using a new transceiver supporting the new band. The proposed system enables the use of state-of-the-art transceivers that support only conventional bands for new wavelength band transmission and reduces the number of transceiver type, thereby reducing additional operational complexity in installation, channel upgrades, and inventory management for multi-band WDM systems.

When we implement a multi-band WDM transmission using a wavelength converter, there is a concern that the transmission performance may be deteriorates due to an increase in noise induced by the wavelength converter itself and noise generated by an optical amplifier added to compensate for insertion loss of the wavelength converter. To suppress linear noise growth, it is necessary to reduce the optical power attenuation by the wavelength converter. Although optical amplifiers can compensate for optical power attenuation, it is important to reduce the number of optical amplifiers as much as possible in multi-band WDM transmission because optical amplifiers that are inferior to conventional erbium-doped fiber amplifiers (EDFAs) may cause significant reach degradation. Therefore, it is important to improve the conversion efficiency of the wavelength converter. Although it is not easy to achieve high efficiency and wide bandwidth at the same time, a 10-THz bandwidth optical parametric amplifier using periodically poled lithium niobate (PPLN) waveguides [13]–[16] is a promising component for wavelength converters by extracting idlers that occur there. In addition, idler generation using the second-order nonlinear polarization is more suitable for batch processing of WDM channels than idler generation using third-order nonlinear polarization because the generation of unwanted nonlinear noise due to the interaction between the WDM channels is exceedingly small.

In this paper, we present the feasibility of S-band WDM transmission using PPLN-based wavelength converters (PPLN-WCs) designed and fabricated in NTT labs to achieve wavelength conversion between C-band and S-band [15], [16]. For this purpose, in addition to the review of subsystem evaluation and system demonstration reported in [17], we describe the definition of the noise figure of the wavelength converter and the estimation results of transmission performance using it. First, we define the conversion efficiency and noise figure of the wavelength converter which are the index for estimating the transmission performance including the wavelength converter. Next, we measure the conversion efficiency and noise figure of the PPLN-WC according to the definition. Finally, we demonstrate S-band WDM transmission without additional S-band optical amplifiers using the evaluated PPLC-WC and C-band real-time transceivers.

2. Characterization of Wavelength Converters

To facilitate estimation of system performance including wavelength converters, it is necessary to characterize linear and nonlinear noise generation in wavelength converters. Since characterization including nonlinear noise is complicated, we first consider only linear noise. For linear noise, we can treat the wavelength converter having low attenuation or gain like an optical amplifier by replacing the gain of the optical amplifier with the conversion efficiency of the wavelength converter. Therefore, the conversion efficiency and noise figure of the wavelength converter are basic parameters required to estimate the system performance.

We define the conversion efficiency of the wavelength converter, η_{wc}, by referring to the definition of gain in [18] as follows.

$$\eta_{\mathrm{wc}} = \frac{P_{\mathrm{out,sig}}(\nu_{\mathrm{idler}}) - P_{\mathrm{out,noise}}(\nu_{\mathrm{idler}})}{P_{\mathrm{in,sig}}(\nu_{\mathrm{probe}}) - P_{\mathrm{in,noise}}(\nu_{\mathrm{probe}})}, \tag{1}$$

where $P_{\mathrm{in,sig}}(\nu_{\mathrm{probe}})$ and $P_{\mathrm{in,noise}}(\nu_{\mathrm{probe}})$ are the input optical power of the signal and noise to the wavelength converter within the WDM channel bandwidth allocated to a probe at frequency ν_{probe}, and $P_{\mathrm{out,sig}}(\nu_{\mathrm{idler}})$ and $P_{\mathrm{out,noise}}(\nu_{\mathrm{idler}})$ are the output optical power of the signal and noise from the wavelength converter within the WDM channel bandwidth allocated to an idler at frequency ν_{idler}. If the signal-to-noise ratio is high enough, the effect of noise is negligible. Note that the conversion efficiency defined here is an output-to-input optical power ratio, rather than the intrinsic efficiency or the energy efficiency of the photon pair in the nonlinear optical medium.

Referring to the noise figure measurement method of optical amplifiers specified in IEC 61290-3-1 [18], the noise figure (NF) of wavelength converters is also the sum of noises due to four noise sources as follows.

$$NF = 10\log\left(F_{\mathrm{shot,sig}} + F_{\mathrm{shot,ase}} + F_{\mathrm{sig\text{-}sp}} + F_{\mathrm{sp\text{-}sp}}\right), \tag{2}$$

where $F_{\mathrm{shot,sig}}$ is the shot noise of the optical signal, $F_{\mathrm{shot,ase}}$ is the shot noise of the amplified spontaneous emission (ASE), $F_{\mathrm{sig\text{-}sp}}$ is the beat noise between the optical signal and the ASE, and $F_{\mathrm{sp\text{-}sp}}$ is the beat noise between the ASE and the ASE. We modified four factors for polarization-multiplexed converted signals from the wavelength-preserving optical amplification in [18] to wavelength conversion by replacing the output to idler:

$$F_{\mathrm{shot,sig}} = \frac{1}{\eta_{\mathrm{wc}}}, \tag{3}$$

$$F_{\mathrm{shot,ase}} = \frac{P_{\mathrm{ase}}(\nu_{\mathrm{idler}})}{\eta_{\mathrm{wc}}^2 P_{\mathrm{in,sig}}(\nu_{\mathrm{probe}})}, \tag{4}$$

$$F_{\mathrm{sig\text{-}sp}} = \frac{P_{\mathrm{ase}}(\nu_{\mathrm{idler}})}{h\nu_{\mathrm{idler}}\eta_{\mathrm{wc}}\Delta\nu}, \tag{5}$$

and

$$F_{\mathrm{sp\text{-}sp}} = \frac{P_{\mathrm{ase}}(\nu_{\mathrm{idler}})^2}{2h\nu_{\mathrm{idler}}\eta_{\mathrm{wc}}^2 P_{\mathrm{in,sig}}(\nu_{\mathrm{probe}})\Delta\nu}, \tag{6}$$

where P_{ase} is the optical power of ASE generated in the wavelength converter, $\Delta\nu$ is the frequency bandwidth of channel slot, and h is the Planck constant. In many cases, the noise figure of the optical amplifier can be calculated only from the beat noise between the optical signal light and the ASE. However, all noise factors are considered here. This is because the shot noise of the optical signal is large in the operating condition in which the gain is not sufficiently large. Since the output optical power of the noise $P_{\text{out,noise}}(\nu_{\text{idler}})$ measured using the optical spectrum analyzer includes the noise associated with the input signal $P_{\text{in,noise}}(\nu_{\text{probe}}, \nu_{\text{probe}})$, they are subtracted as follows.

$$P_{\text{ase}}(\nu_{\text{idler}}) = P_{\text{out,noise}}(\nu_{\text{idler}}) - \eta_{wc} P_{\text{in,noise}}(\nu_{\text{probe}}) \\ - GP_{\text{in,noise}}(\nu_{\text{idler}}) \quad (7)$$

where G is the parametric gain. $P_{\text{in,noise}}(\nu_{\text{idler}})$ is added from the definition in [18]. However, it would be negligibly small because there is a filter before processing in a typical inter-band application. Note, however, that the output noise at the idler wavelength depends not only on the signal and noise power inputs at the probe wavelength, but also on the input noise at the idler wavelength. The optical power of the ASE is obtained by substituting the measured value by the optical spectrum analyzer into (7). The obtained ASE optical power is substituted into (3)–(6) to obtain the noise factors, from which the noise figure of the wavelength converter is calculated by (2).

The system performance including the wavelength converter can be estimated by using the conversion efficiency and noise figure. However, if the wavelength converter is operated in the condition where nonlinear noise generation is not negligible, additional characterization of the nonlinear noise is required to estimate system performance accurately. Although GN model [19] consider the impact of nonlinear noise, it should be noted that the nonlinear noise generated in wavelength converter is not necessarily a result of statistical randomization due to chromatic dispersion [20].

3. Preliminary Evaluation of PPLN-Based Wavelength Converter

Two sets of PPLN-based wavelength converters (PPLN-WC-1 and PPLN-WC-2), shown in Fig. 2, were evaluated for the purpose of demonstrating WDM transmission in S-band by inserting them after and before the C-band WDM transceiver. The PPLN-WC consists of two PPLN differential frequency generators (DFG$_x$ and DFG$_y$), a laser diode (LD) for the fundamental pump source, two PPLN second harmonic generators (SHG$_x$ and SHG$_y$), two polarization beam splitters (PBS$_{\text{in}}$ and PBS$_{\text{out}}$), and an optical delay line (ODL). A 2-W amplified fundamental pump light with a wavelength between the C- and S-band ($\nu_{\text{f}} = 196.200$ THz, 1527.99 nm in wavelength) was used. The phase-matching condition of the PPLN waveguide for SHG was thermally adjusted to maximize the output of the second harmonic pump light ($\nu_{\text{sh}} = 392.400$ THz, 764.00 nm in wavelength). At an input end and an output end of the PPLN waveguide for DFGs,
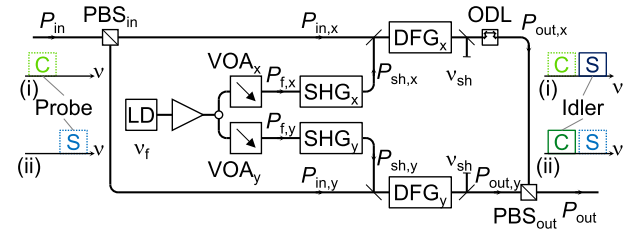

Fig. 2 Configuration of the PPLN-based wavelength converter consisted of differential frequency generators (DFGs) sandwiched by polarization beam splitters (PBSs), a fundamental pump source laser diode (LD), second harmonic generators (SHGs), and an optical delay line (ODL).

filters for combining and dividing a C+S-band WDM signal and a second harmonic pump light (ν_{sh}) were arranged. Since the parametric process is sensitive to the polarization state of the input signal, DFG$_x$ and DFG$_y$ were inserted into two polarization diversity paths sandwiched between PBS$_{\text{in}}$ and PBS$_{\text{out}}$. The two optical path lengths were matched using ODL to avoid addition of the first order polarization mode dispersion after combining each polarization component.

An emulated WDM signal was input to the PPLN-WC to uniformly adjust the conversion efficiency for each WDM channel. The WDM signal were 75-GHz spaced 64 channels, ranging from 191.375 THz to 196.100 THz, with each channel having a bandwidth of 30 GHz and uniform optical power, generated using an ASE source and a wavelength selective switch (WSS) in the experimental setup shown in the next section. The optical power deviation of the output idler between channels was reduced by adjusting the temperature of the PPLN waveguide for each DFG. The fundamental pump power inputs to each SHG, $P_{\text{f,x}}$ and $P_{\text{f,y}}$, were adjusted by variable optical attenuators (VOA$_x$ and VOA$_y$) so that the conversion efficiencies were the same for the two polarization diversity paths, and unity in total power, $\eta_{\text{wc}} = 1$. Then, $P_{\text{f,x}} = 28$ dBm and $P_{\text{f,y}} = 27$ dBm, and the efficiency of each SHG, $P_{\text{sh}}/P_{\text{f}}$, was approximately -3 dB. SHG$_x$ needed slightly higher pump power to compensate for the loss of ODL in the same path.

First, the reversible spectral inversion shown in Fig. 3 was confirmed by launching a C-band WDM signal and an S-band WDM signal generated by the other PPLN-WC into the PPLN-WC. Gain at the probe, conversion efficiency at the idler, and noise figure at the probe and idler were calculated by the method described in Sect. 2 using the input and output optical spectra of each PPLN-WC at a sufficiently low optical power input of 0 dBm (-18 dBm/ch), and the C-band and S-band input cases were plotted in Figs. 4 and 5, respectively. It was confirmed that PPLN-WC-1 and PPLN-WC-2 had the same characteristics for both conversions. The inter-channel deviations of the conversion efficiency in the C-to-S and S-to-C conversions were 1.5 dB and 2.0 dB, respectively. The difference in conversion efficiency between the two polarization diversity paths inducing polarization-dependent loss in each channel was less than 1.0 dB under all conditions. The average noise figure of the probe and idler channels for the C-to-S (S-to-C) conversion were 4.5 dB (4.5 dB) and 5.7 dB
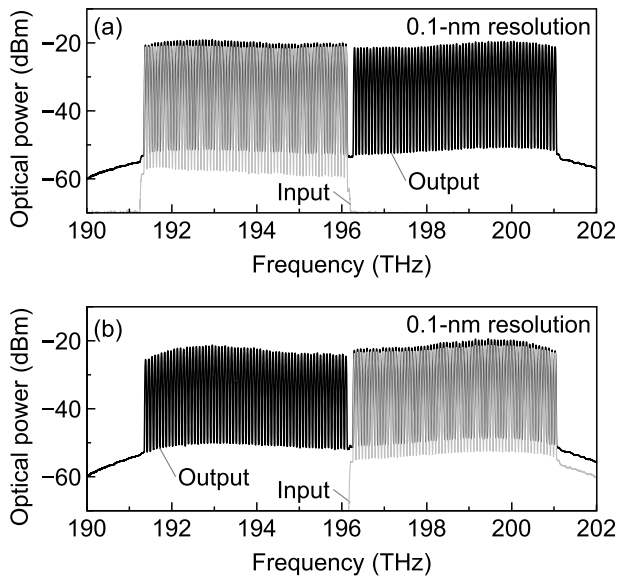
Fig. 3 Input optical spectrum of 64 channel WDM signal to PPLN-based wavelength converter (gray line) and its output optical spectrum (black line) in (a) C-to-S conversion and (b) S-to-C conversion.
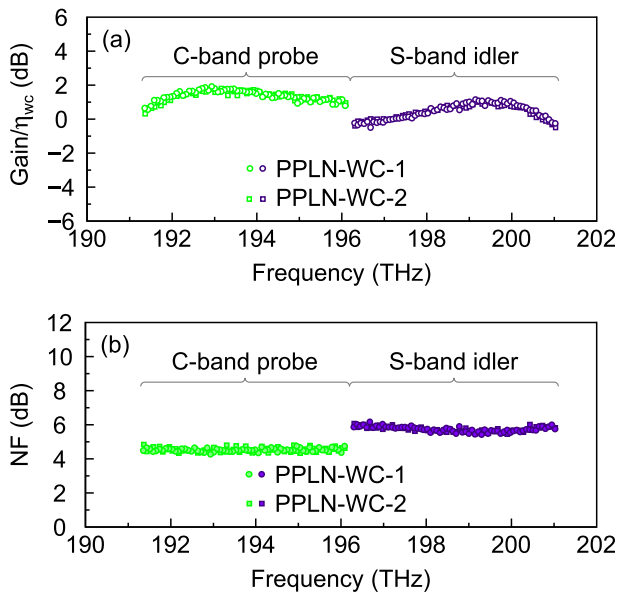

Fig. 4 (a) Gain/conversion efficiency and (b) noise figure of both probe and idler through PPLN-WC-1 and PPLN-WC-2 in C-to-S conversion at 64 channel WDM input (−18 dBm/ch).

Fig. 5 (a) Gain/conversion efficiency and (b) noise figure of both probe and idler through PPLN-WC-1 and PPLN-WC-2 in S-to-C conversion at 64 channel WDM input (−18 dBm/ch).

Fig. 6 Input optical power dependence of the conversion efficiency of PPLN-WC-1 for single-channel and 64 channel WDM signal.

conversion efficiency is decreased when a high optical power not sufficiently lower than that of pump is input. In such a saturation region, the output optical power reduction and signal distortion may occur, so that we evaluated the saturation characteristic. As shown in Fig. 6, the average conversion efficiency was constant in the range of input optical power below +10 dBm and degraded as the input optical power increased. The saturation of the conversion efficiency for the 64 channel WDM and single channel showed the same trend, suggesting that it is determined by the total power rather than the power per channel.

4. Transmission Experiment

We constructed an experimental setup to test S-band WDM transmission converted by the PPLN-WC with C-band real-time transceivers as shown in Fig. 7. A 400-Gb/s signal with 64-GBd dual-polarization (DP)-16QAM modulation format output from a C-band real-time transceiver was used as a test channel. A 64 channel WDM signal with 75-GHz spacing in C-band was generated by combining a single 400-Gb/s

(6.0 dB), respectively. The slightly larger deviation of the conversion efficiency and noise figure in the S-to-C conversion was due to the wavelength-dependent loss of ODL increasing at longer wavelengths.

Next, the dependence of the conversion efficiency of PPLN-WC-1 on the input optical power was measured using a single-channel transceiver output at 193.400 THz and a 64 channel WDM signal shown in Fig. 3(a). Although the wavelength converter before transmission requires a high optical output to avoid the addition of an optical amplifier, the
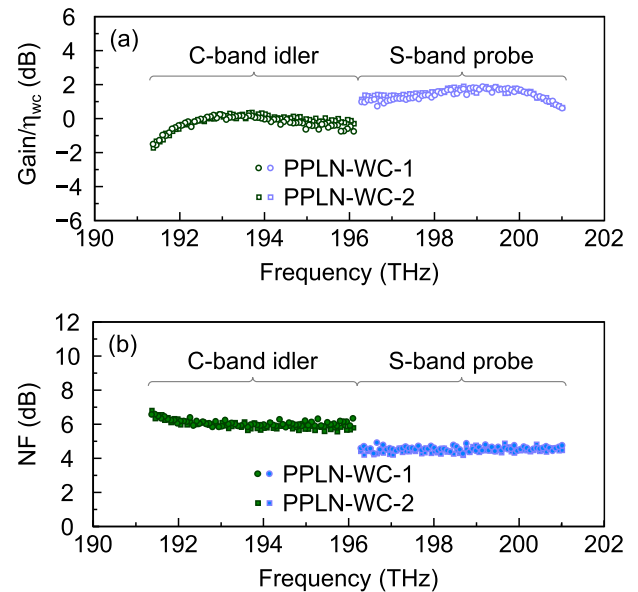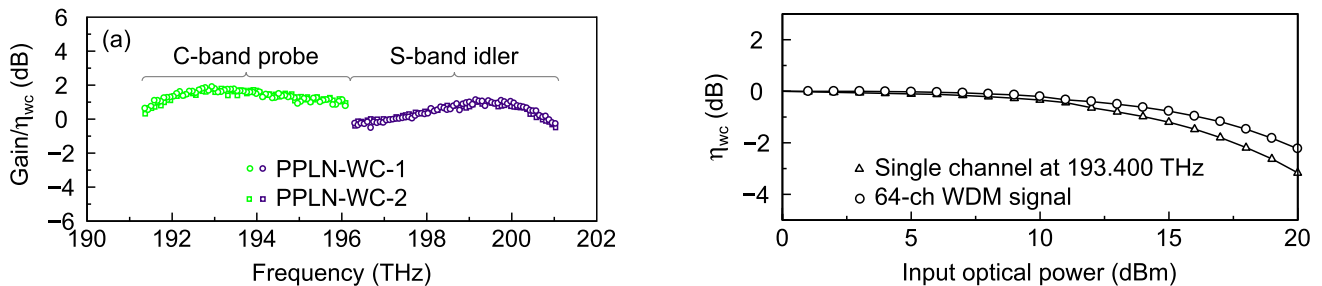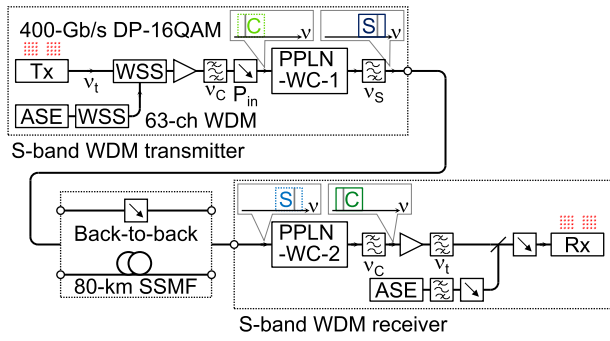
Fig. 7 Experimental setup for S-band WDM transmission consisted of transceivers (Tx, Rx), wavelength-selective switches (WSSs), amplified spontaneous emission sources (ASEs), and PPLN-based wavelength converters (PPLN-WCs), and a standard single-mode fiber (SSMF).

Fig. 8 Penalty in optical signal-to-noise ratio (OSNR) at the working range limit of forward error correction of 400-Gb/s DP-16QAM signal at 193.4 THz without transmission for various optical input power to the PPLN-WC-1 for single channel case and 64 channel WDM case.

Fig. 9 Estimated reachable distance for each WDM channel calculated from the measured conversion efficiency and noise figure for various optical input power to the PPLN-WC-1.

signal with the other channels of the spectrally shaped ASE to provide the same optical power per channel. The conversion efficiencies of PPLN-WC-1 and PPLN-WC-2 were set to unity at 0-dBm input. The C-band WDM signal was converted to S-band by PPLN-WC-1, and the S-band WDM signal was extracted by an optical filter with an insertion loss of 2.2 dB to remove ASE around the fundamental pump wavelength. The converted S-band WDM signal after transmission was reverted to the C-band by PPLN-WC-2, and the C-band WDM signal was extracted by an optical filter. The channel under test was extracted with a 1-nm optical filter after amplification and input to the receiver with regulated optical power. In addition, an ASE was loaded in front of the receiver to measure the penalty in the optical signal-to-noise ratio (OSNR) caused by signal distortion that would occur in the wavelength converter. The signal quality is evaluated by monitoring the value output from the receiver using digital coherent detection [21].

First, the OSNR penalty at the working range limit of forward error correction (FEC) for high optical power input to PPLN-WC-1 was measured in a back-to-back configuration. Transceiver outputs at $\nu_t = 193.400$ THz were evaluated with/without ASE surrounding channels. To investigate the effect of signal distortion due to saturation of conversion efficiency on only the PPLN-WC-1, the input optical power to the PPLN-WC-2 was adjusted to 0 dBm, which is assumed to be sufficiently low to avoid the saturation. As shown in Fig. 8, in the case of a single channel, the OSNR penalty increases as the input optical power increases, and in the case of a WDM signal, the OSNR penalty is exceedingly small even at +20 dBm (+2 dBm/ch), although the influence of nonlinear distortion in the idler generation process can be observed slightly. From this result, it was confirmed that when a 64 channel WDM signal with uniform channel power is input to the PPLN-WC, although the output optical power decreases due to saturation of the conversion efficiency, no significant signal distortion occurs when the total input optical power to the PPLN-WC is below +20 dBm.

Using the conversion efficiency and noise figure evaluated in Sect. 3, the reachable distance in the experimental setup in Fig. 7 was estimated. The loss coefficient of the
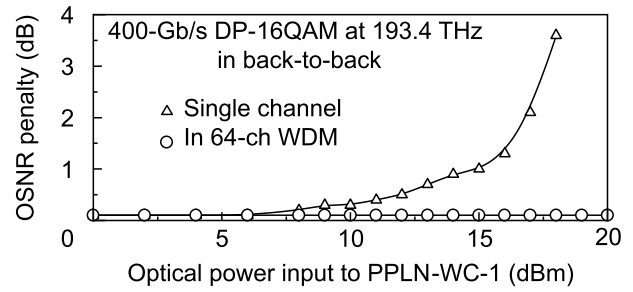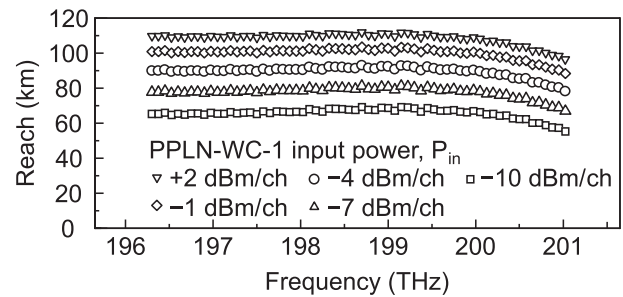
transmission fiber, which is a standard single-mode fiber (SSMF) compliant with G.652.D used in the experimental setup, was 0.22–0.24 dB/km in the range of 196.3–201.0 THz from the fiber loss measurement. The measured conversion efficiency including the saturation and noise figure for each channel were applied to the estimation as the characterized value of the wavelength converter. The loss between the transmitter and the C-band EDFA and noise figure of C-band EDFA were 10.0 dB and 6.8 dB, respectively. The required OSNR for error free operation after FEC decoding was set to 21.8 dB, which corresponds to the 400-Gb/s DP-16QAM of the transceiver used, assuming a noise level with a resolution bandwidth of 0.1 nm. In practice, as the fiber input optical power increases, nonlinear noise in the transmission fiber due to inter-channel interactions increases, and inter-channel stimulated Raman scattering (SRS) increases the loss of short wavelength channels, and decreases the loss of long wavelength channels, which are not considered here. Figure 9 shows the results calculated by changing the input optical power to the PPLN-WC-1. As the input power to the PPLN-WC-1 increases, the reachable distance increases, but the increase in the reach gradually decreases because the fiber input power decreases due to saturation of the conversion efficiency of the wavelength converter. In short wavelength channels, the S-to-C converter has a large noise figure and high fiber loss, so the reach tends to be short. Although it is necessary to pay attention to the generation of nonlinear noise in the transmission fiber, it is not so serious in the
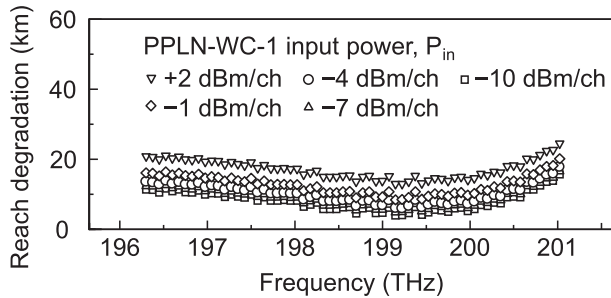
Fig. 10 Reach degradation due to the introduction of wavelength converters for various optical input power to the PPLN-WC-1.

Fig. 11 Bit error ratio (BER) before forward error correction (FEC) decoding through 80-km transmission of typical channels in 64 channel WDM signal plotted with markers for measured value and lines for calculated estimation.

present calculation range of below +2 dBm/ch. From the calculation result, it was found that sufficient OSNR could be obtained in all channels in the SSMF transmission of 80 km, though it was difficult to obtain sufficient OSNR in the short wavelength channel for longer distance. Figure 10 shows the reach degradation due to the wavelength converter, calculated by taking the difference between the practical reach in Fig. 9 and the ideal one assuming both the conversion efficiency and the noise figure of 0 dB. This result simply shows how much the introduction of the wavelength converter degrades signal quality when the performance of transceivers and optical amplifiers are the same in the C-band and S-band. However, since the performance of the S-band optical component may not reach the performance of the C-band [10], the adoption of the wavelength converter is not necessarily disadvantageous compared to the use of the S-band optical component.

Next, from the above reach estimation including measured noise figure and OSNR penalty of the PPLN-WC, we used 80-km SSMF as the transmission line and its loss was 17.8–19.2 dB within 196.3–201.0 THz. The pre-FEC bit error ratio (BER) of the test channel was measured by counting the number of corrected bit in the absence of uncorrected errors in the receiver digital signal processing when the center channel (ν_t = 193.400 THz, 199.000 THz at transmission), the near edge channel (ν_t = 196.100 THz, 196.300 THz at transmission) or the far edge channel (ν_t = 191.375 THz, 201.025 THz at transmission) within 64 channels in the C-band with transceiver output. The measured pre-FEC BER was plotted as a marker in Fig. 11 together with a line indicating the calculated estimation. The estimated value was obtained by combining the receiver OSNR obtained in the derivation process of Fig. 9 with the OSNR dependence of the BER at the transmitter/receiver direct connection. Therefore, the estimation lacks the nonlinear distortion occurred in the transmission fiber. There was no residual bit error for each plot after decoding of 23% and 20% mixed soft-decision FEC, and the measured values agreed with the estimation in the linear transmission region. Due to the limitations of the components used in the setup, measurements were possible only at input optical power below +2 dBm/ch to the PPLN-WC-1. Assuming multi-band transmission such as S+C+L-band, the measurement range is reasonable because
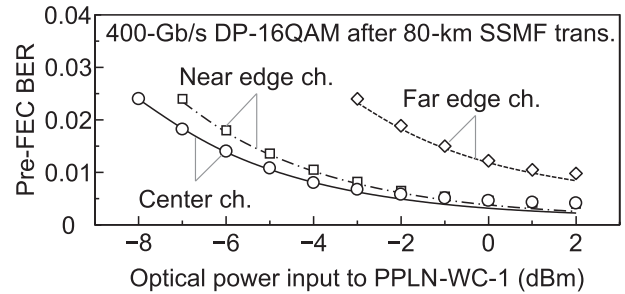
the spectral tilt caused by inter-channel SRS is significantly larger at higher optical power fiber inputs [22].

5. Conclusion

We reviewed the experimental demonstration of S-band WDM transmission using PPLN-based wavelength converter and C-band real-time transceiver reported in [17]. In addition, we explicitly defined the conversion efficiency and noise figure in the wavelength converter and the estimated reachable distance using them were presented together with the experimental results.

As a preliminary step of multi-band WDM transmission, the PPLN-based wavelength converter to achieve WDM transmission in S-band in combination with the C-band transceiver was evaluated and applied to the S-band transmission system demonstration. Using the PPLN-WC with uniform optical power preserving conversion covering whole C-band, we demonstrated the post-FEC error-free transmission with 80-km SSMF of real-time 400-Gb/s DP-16QAM signal by replacing typical channels within the emulated 75-GHz spaced 64-ch WDM signal in S-band without using additional S-band optical amplifier. Although signal distortion due to saturation of conversion efficiency was a concern, no significant degradation was observed under the test conditions. It was confirmed that the transmission performance degradation by the introduction of the wavelength converter is dominated by the linear noise, and that the transmission system can be constructed without additional consideration of the nonlinear noise.

Based on this result, we conducted an additional study combining the C+L-band system and the demonstrated system. We verified the same distance transmission in S+C+L-band simultaneous transmission and achieved capacity enhancement [23]. As a result, it has been verified that the wavelength conversion technology is effective for the realization of a multi-band WDM system, though it is still limited to a single span transmission.

To extend the transmission distance in a multi-band WDM system using a wavelength band exceeding 100 nm, it is essential to optimize the in-band and inter-band optical power in consideration of the optical power transfer by inter-

channel SRS. In addition, the effective technology for the S-band amplification will contribute to the realization of a large capacity without the significant reduction of the transmission distance.

Acknowledgments

References

[1] J. Kani, K. Hattori, M. Jinno, T. Kanamori, and K. Oguchi, "Triple-wavelength-band WDM transmission over cascaded dispersion-shifted fibers," IEEE Photon. Technol. Lett., vol.11, no.11, pp.1506–1508, Nov. 1999. DOI: 10.1109/68.803094

[2] K. Fukuchi, T. Kasamatsu, M. Morie, R. Ohhira, T. Ito, K. Sekiya, D. Ogasahara, and T. Ono, "10.92-Tb/s (273 × 40-Gb/s) triple-band/ultra-dense WDM optical-repeatered transmission experiment," Proc. Opt. Fiber Commun. Conf., PD24, Anaheim, CA, USA, March 2001.

[3] T. Tanaka, K. Torii, M. Yuki, H. Nakamoto, T. Naito, and I. Yokota, "200-nm bandwidth WDM transmission around $1.55 \mu m$ using distributed Raman amplifier," Proc. 28th Eur. Conf. Opt. Commun., PD4.6, Copenhagen, Denmark, Sept. 2002.

[4] B.J. Puttnam, R.S. Luís, G. Rademacher, M. Mendez-Astudilio, Y. Awaji, and H. Furukawa, "S, C and extended L-band transmission with doped fiber and distributed Raman amplification," Proc. Opt. Fiber Commun. Conf., Th4C.2, San Francisco, CA, USA, June 2021. DOI: 10.1364/OFC.2021.Th4C.2

[5] L. Galdino, A. Edwards, W. Yi, E. Sillekens, Y. Wakayama, T. Gerard, W.S. Pelouch, S. Barnes, T. Tsuritani, R.I. Killey, D. Lavery, and P. Bayvel, "Optical fibre capacity optimisation via continuous bandwidth amplification and geometric shaping," IEEE Photon. Technol. Lett., vol.32, no.17, pp.1021–1024, Sept. 2020. DOI: 10.1109/LPT.2020.3007591

[6] F. Hamaoka, K. Minoguchi, T. Sasai, A. Matsushita, M. Nakamura, S. Okamoto, E. Yamazaki, and Y. Kisaka, "150.3-Tb/s ultra-wideband (S, C, and L bands) single-mode fibre transmission over 40-km using >519 Gb/s/λ PDM-128QAM signals," Proc. 44th Eur. Conf. Opt. Commun., 2018, Mo4G.1. DOI: 10.1109/ECOC.2018.8535140

[7] A. Arnould, A. Ghazisaeidi, D. Le Gac, P. Brindel, M. Makhsiyan, K. Mekhazni, F. Blache, N. Fontaine, D. Neilson, R. Ryf, H. Chen, M. Achouche, and J. Renaudier, "103 nm ultra-wideband hybrid Raman/SOA transmission over $3 \times 100\,km$ SSMF," J. Lightw. Technol., vol.38, no.2, pp.504–508, Jan. 2020. DOI: 10.1109/JLT.2019.2946590

[8] X. Zhao, S. Escobar-Landero, D. Le Gac, A. Lorences-Riesgo, T. Viret-Denaix, Q. Guo, L. Gan, S. Li, S. Cao, X. Xiao, N.E. Dahdah, A. Gallet, S. Yu, H. Hafermann, L. Godard, R. Brenot, Y. Frignac, and G. Charlet, "200.5 Tb/s transmission with S+C+L amplification covering 150 nm bandwidth over $2\times100\,km$ PSCF spans," Proc. 48th Eur. Conf. Opt. Commun., Th3C.4, Basel, Switzerland, Sept. 2022.

[9] T. Hoshida, V. Curri, L. Galdino, D.T. Neilson, W. Forysiak, J.K. Fischer, T. Kato, and P. Poggiolini, "Ultrawideband systems and networks: Beyond C+L-band," Proc. IEEE, vol.110, no.11, pp.1725–1741, Nov. 2022. DOI: 10.1109/JPROC.2022.3202103

[10] R. Emmerich, M. Sena, R. Elschner, C. Schmidt-Langhorst, I. Sackey, C. Schubert, and R. Freund, "Enabling S-C-L-band systems with standard C-band modulator and coherent receiver using nonlinear predistortion," J. Lightw. Technol., vol.40, no.5, pp.1360–1368, March 2022. DOI: 10.1109/JLT.2021.3123430

[11] M.S. Sarwar, T. Sakamoto, T. Kato, and T. Hoshida, "TransLambda: A multi-band transmission system and its realization, practical applications and use cases in optical networks," Proc. Opt. Fiber Commun. Conf., M2G.6, San Diego, CA, USA, March 2020. DOI: 10.1364/OFC.2020.M2G.6

[12] T. Kato, S. Watanabe, T. Yamauchi, G. Nakagawa, H. Muranaka, Y. Tanaka, Y. Akiyama, and T. Hoshida, "Real-time transmission of 240×200-Gb/s signal in S+C+L triple-band WDM without S- or L-band transceivers," Proc. 45th Eur. Conf. Opt. Commun., PD1.7, Dublin, Ireland, Sept. 2019. DOI: 10.1049/cp.2019.1021

[13] T. Kobayashi, S. Shimizu, M. Nakamura, T. Umeki, T. Kazama, R. Kasahara, F. Hamaoka, M. Nagatani, H. Yamazaki, H. Nosaka, and Y. Miyamoto, "Wide-band inline-amplified WDM transmission using PPLN-based optical parametric amplifier," J. Lightw. Technol., vol.39, no.3, pp.787–794, Feb. 2021. DOI: 10.1109/JLT.2020.3039192

[14] S. Shimizu, T. Kazama, T. Kobayashi, T. Umeki, K. Enbutsu, T. Kashiwazaki, R. Kasahara, K. Watanabe, and Y. Miyamoto, "Inter-band non-degenerate phase-sensitive amplification scheme for low-noise full C-band transmission," IEICE ComEX, vol.11, no.1, pp.64–69, Nov. 2021. DOI: 10.1587/comex.2021XBL0184

[15] S. Shimizu, T. Kobayashi, T. Kazama, T. Umeki, M. Nakamura, K. Enbutsu, T. Kashiwazaki, R. Kasahara, K. Watanabe, and Y. Miyamoto, "PPLN-based optical parametric amplification for wide-band WDM transmission," J. Lightw. Technol., vol.40, no.11, pp.3374–3384, June 2022. DOI: 10.1109/JLT.2022.3142749

[16] T. Kobayashi, S. Shimizu, M. Nakamura, T. Umeki, T. Kazama, J. Yoshida, S. Takasaka, Y. Tatamida, H. Kawakami, F. Hamaoka, M. Nagatani, H. Yamazaki, K. Watanabe, T. Saida, and Y. Miyamoto, "50-Tb/s (1 Tb/s $\times$ 50 ch) WDM transmission on two 6.25-THz bands using hybrid inline repeater of PPLN-based OPA and incoherent-forward-pumped DRA," Proc. Opt. Fiber Commun. Conf., Th4A.8, San Diego, CA, USA, March 2022. DOI: 10.1364/OFC.2022.Th4A.8

[17] T. Kato, H. Muranaka, Y. Tanaka, Y. Akiyama, T. Hoshida, S. Shimizu, T. Kobayashi, T. Kazama, T. Umeki, K. Watanabe, and Y. Miyamoto, "WDM transmission in S-band using PPLN-based wavelength converters and 400-Gb/s C-band real-time transceivers," Proc. 27th OptElectron. Commun. Conf., WA-3-4, Toyama, Japan, July 2022. DOI: 10.23919/OECC/PSC53152.2022.9849997

[18] "Optical Spectrum Analyzer Operation Manual," Antisu Corporation, https://dl.cdn-anritsu.com/en-au/test-measurement/files/Manuals/Operation-Manual/MS9740B/MS9740B_Operation_Manual_e_4_0.pdf, accessed Dec. 8. 2022.

[19] P. Poggiolini, G. Bosco, A. Carena, V. Curri, Y. Jiang, and F. Forghieri, "The GN-model of fiber non-linear propagation and its applications," J. Lightw. Technol., vol.32, no.4, pp.694–721, Feb. 2014. DOI: 10.1109/JLT.2013.2295208

[20] V. Oliari, E. Agrell, and A. Alvarado, "Regular perturbation on the group-velocity dispersion parameter for nonlinear fibre-optical communications," Nat. Commun., vol.11, Article number 933, Feb. 2020. DOI: 10.1038/s41467-020-14503-w

[21] "1FINITY T700 Transport Blade," Fujitsu Network Communications, https://marketing.us.fujitsu.com/rs/407-MTR-501/images/1FINITYT700dsR20.1.2.pdf, accessed March 30. 2023.

[22] D. Semrau, L. Galdino, E. Sillekens, D. Lavery, R.I. Killey, and P. Bayvel, "Modulation format dependent, closed-form formula for estimating nonlinear interference in S+C+L band systems," Proc. 45th Eur. Conf. Opt. Commun., W.1.D.1, Dublin, Ireland, Sept. 2019. DOI: 10.1049/cp.2019.0892

[23] T. Kato, H. Muranaka, Y. Tanaka, Y. Akiyama, T. Hoshida, S. Shimizu, T. Kobayashi, T. Kazama, T. Umeki, K. Watanabe, and Y. Miyamoto, "S+C+L-band WDM transmission using 400-Gb/s real-time transceivers extended by PPLN-based wavelength converter," Proc. 48th Eur. Conf. Opt. Commun., We4D.4, Basel, Switzerland, 2022.

Tomoyuki Kato received the B.E., M.E., and Dr.Eng. degrees in electronic engineering from Yokohama National University, Yokohama, Japan, in 2001, 2003, and 2006, respectively. From 2006 to 2009, he was a Research Associate with the Precision and Intelligence Laboratories, Tokyo Institute of Technology, Tokyo, Japan. Since he joined Fujitsu Laboratories Ltd., Kawasaki, Japan, in 2009, he has been engaged in the research of nonlinear optical signal processing for dense wavelength-division multiplexing optical transmission systems. Since 2019, he has been with Fujitsu Ltd. Dr. Kato is a member of IEEE Photonics Society. He served on the Technical Program Committees for the OptoElectronics and Communications Conference (OECC) and the European Conference on Optical Communication (ECOC).

Hidenobu Muranaka received the B.S. and M.S. degrees in Electrical Engineering from Hokkaido University in 2004 and 2006, respectively. He joined Fujitsu Laboratories Ltd., Atsugi, Japan in 2006. His research activities cover optical assembly, packaging technologies, and so on. Recent his research interests in the area of optical network. He is a member of the Institute of Electronics, Information, and Communication Engineers of Japan (IEICE).

Yu Tanaka received the Ph.D. degree in material science from the Tokyo Institute of Technology, Tokyo, Japan, in 2000. In 2002, he joined Fujitsu Laboratories Ltd., Atsugi, Japan. Since then, he has been involved in the development of optical devices including quantum dot lasers and crystal-based photonic switches. In 2012, he joined the Photonics Electronics Technology Research Association, where he is currently a Senior Researcher. He is currently engaged in the development and industrialization of integrated silicon-photonics-based optical transceivers. Dr. Tanaka is a member of the Institute of Electronics, Information, and Communications Engineers of Japan.

Yuichi Akiyama received the B.E. and M.E. degrees in electrical and electronics engineering from Sophia University, Tokyo, Japan, in 1994 and 1996, respectively. In 1996, he joined the Optoelectronic Systems Laboratory, Fujitsu Laboratories Ltd., Japan. He is currently working with Fujitsu Ltd., Kawasaki, Japan, where he has been engaged in the research and development of wavelength-division multiplexing optical transmission systems. Mr. Akiyama is a member of the Institute of Electronics, Information, and Communications Engineers of Japan.

Takeshi Hoshida received the B.E., M.E., and Ph.D. degrees in electronic engineering from The University of Tokyo, Tokyo, Japan, in 1993, 1995, and 1998, respectively. Since he joined Fujitsu Laboratories Ltd., Kawasaki, Japan, in 1998, he has been engaged in the research and development of dense WDM optical transmission systems. From 2000 to 2002, he was with Fujitsu Network Communications, Inc., Richardson, TX, USA. Since 2007, he has been with Fujitsu Ltd., Kawasaki, Japan, and he currently heads Fujitsu's optical transmission research efforts. Dr. Hoshida is a Senior Member of the Institute of Electronics, Information and Communication Engineers (IEICE) and a member of the Japan Society of Applied Physics (JSAP). He received the Commendation for Science and Technology by the Ministry of Education, Culture, Sports, Science and Technology (Awards for Science and Technology in Development Category) in 2020 and the Japan Patent Office Commissioner Award of the National Commendation for Invention in 2020.

Shimpei Shimizu received the B.E. degree in engineering and the M.E. degree in information science and technology from Hokkaido University, Sapporo, Japan, in 2016 and 2018, respectively. He joined the NTT Network Innovation Laboratories, Yokosuka, Japan, in 2018. He is a member of the Institute of Electronics, Information and Communication Engineers (IEICE) of Japan and the IEEE Photonics Society.

Takayuki Kobayashi received the B.E., M.E., and Dr. Eng. degrees from Waseda University, Tokyo, Japan, in 2004, 2006, and 2019, respectively. In April 2006, he joined the NTT Network Innovation Laboratories, Yokosuka, Japan, where he was engaged in the research on high-speed and high-capacity digital coherent transmission systems. In April 2014, he moved to the NTT Access Network Service Systems Laboratories, Yokosuka, and was engaged in 5G mobile optical network systems. Since July 2016, he moved back to the NTT Network Innovation Laboratories and has been working on high-capacity optical transmission systems. His current research interests are long-haul optical transmission systems employing spectrally efficient modulation formats enhanced by digital and optical signal processing. He is a member of the Institute of Electronics, Information and Communication Engineers (IEICE) of Japan. He has been served as a Technical Program Committee (TPC) Member of the Electrical Subsystems' Category for the Optical Fiber Communication Conference (OFC) from 2016 to 2018. He has been serving as a TPC Member of the "Point-to-Point Optical Transmission" Category for the European Conference on Optical Communication (ECOC) since 2018.

Takushi Kazama received the B.S. and M.S. degrees in electrical engineering from The University of Tokyo, Tokyo, Japan, in 2009 and 2011, respectively. In 2011, he joined the NTT Device Technology Laboratories, Japan, where he has been engaged in research on nonlinear optical devices based on periodically poled LiNbO3 waveguides. He is a member of the Institute of Electronics, Information, and Communication Engineers of Japan (IEICE) and the Japan Society of Applied Physics (JSAP).

Takeshi Umeki received the B.S. degree in physics from Gakusyuin University, Tokyo, Japan, in 2002, and the M.S. degree in physics and the Ph.D. degree in nonlinear optics from The University of Tokyo, Tokyo, in 2004 and 2014, respectively. He joined the NTT Photonics Laboratories, Atsugi, Japan, in 2004, since then he has been involved in research on nonlinear optical devices based on periodically poled LiNbO3 waveguides. He is a member of the Japan Society of Applied Physics (JSAP), the Institute of Electronics, Information, and Communication Engineers (IEICE), and the IEEE/Photonics Society.

Kei Watanabe received the B.E., M.E., and Dr. Eng. degrees in physical electronics from Kobe University, Kobe, Japan, in 1998, 2000, and 2003, respectively. In 2004, he joined NTT Laboratories, Kanagawa, Japan, where he engaged in research on silica-based optical waveguides. From 2008 to 2009, he was a Visiting Researcher with Photonic Research Group, Ghent University, Ghent, Belgium, where he focused on uniting silicon photonics and silica-based optical waveguides. Since 2009, he has been engaged in the development of InP-based high-speed Mach-Zehnder modulators. He is a Member of the Japan Society of Applied Physics, the Institute of Electronics, Information, and Communication Engineers of Japan, and IEEE Photonics Society.

Yutaka Miyamoto received the B.E. and M.E. degrees in electrical engineering from Waseda University, Tokyo, Japan, in 1986 and 1988, respectively, and the Dr. Eng. degree in electrical engineering from Tokyo University, Tokyo, in 2016. He joined the NTT Transmission Systems Laboratories, Yokosuka, Japan, in 1988, where he was engaged in the research and development of highspeed optical communications systems including the 10-Gbit/s first terrestrial optical transmission system (FA-10G) using erbium-doped fiber amplifiers (EDFA) inline repeaters. He was with the NTT Electronics Technology Corporation, Yokohama, Japan, from 1995 to 1997, where he was engaged in the planning and product development of high-speed optical module at the data rate of 10 Gb/s and beyond. Since 1997, he has been with the NTT Network Innovation Laboratories, Yokosuka, where he has contributed to the research and development of optical transport technologies based on 40/100/400-Gbit/s channel and beyond. He is currently an NTT Fellow and the Director of the Innovative Photonic Network Research Center, NTT Network Innovation Laboratories, where he has been investigating and promoting the future scalable optical transport network with the Pbit/s-class capacity based on innovative transport technologies such as digital signal processing, space division multiplexing, and cutting-edge integrated devices for photonic preprocessing. He is a fellow of the Institute of Electronics, Information and Communication Engineers (IEICE).